Accurate predictions of ionization and atomization energies without the Born-Oppenheimer approximation

Yubo Yang,[1] Ilkka Kylänpää,[2, 1] Norm M. Tubman,[1] Jaron T. Krogel,[3]
Michael V. Pak,[4] Sharon Hammes-Schiffer,[4] and David M. Ceperley[1]

[1]*Department of Physics, University of Illinois, Urbana, Illinois 61801 USA*
[2]*Department of Physics, Tampere University of Technology, P.O. Box 692, FI-33101 Tampere, Finland*
[3]*Materials Science & Technology Division, Oak Ridge National Laboratory, Oak Ridge, TN 37831*
[4]*Department of Chemistry, University of Illinois, Urbana, Illinois 61801 USA*
(Dated: April 24, 2015)

In this work we calculate the non-relativistic ground-state energies of first row atoms, their corresponding ions and hydrides both adiabatically and non-adiabatically. For this we utilize the fixed-node diffusion Monte carlo method, in which the so-called dragged-node approximation is used in the non-adiabatic simulations. We report ground state energies, ionization energies and atomization energies to an accuracy of $0.1 - 5.0$mHa. We find the ionization energies of the atoms to be independent of the adiabatic assumption, suggesting that either the energy difference between the adiabatic and non-adiabatic ground states is entirely due to the zero point motion of the nuclei or the coupling between the nucleus and electrons is not important in the ionization process. The atomization energies of simple hydrides, however, are significantly influenced by the non-adiabatic coupling of electrons and nuclei. To this end, we demonstrate the necessity to include non-adiabatic effects for accurate prediction of the properties of simple hydrides. Moreover, further development of the dragged-node approach are discussed by considering a multi-time-step scheme for moving the ions.

I. INTRODUCTION

There has been several recent discoveries that suggest that quantum wave functions, which include both electronic and ionic degrees of freedom, have many interesting properties that have yet to be explored [**refs. here**]. This includes the development of equations that exactly factorize a wave function into electron and ionic components [**refs. here**], the disappearance of conical intersections in wave functions of model systems [**refs. here**], and the use of quantum entanglement to study electronic and ionic density matrices [**refs. here**]. Extending such studies to realistic systems is of broad interest and will considerably expand our understanding of electron-ion systems. However, treatment of *ab initio* electron-ion systems is challenging and applications have thus been limited. The most accurate simulations of electron-ion wave functions are generally done with very specialized wave functions, which are limited to rather small systems sizes.

As a framework to address these problems in general realistic systems, we recently demonstrated that quantum Monte Carlo can be combined with quantum chemistry techniques to treat electron-ion wave functions [1]. We showed that this method can be used to treat realistic systems much larger than previously simulated, and we demonstrated that all of this could be done while maintaing a highly accurate wave function. We extend our previous work by considering the simulation of a large set of atoms and molecules. We calculate ionization energies and dissociation energies which can be directly compared with previous benchmarking results. A new technique which involves multiple time steps for different species in the imaginary time propagator is also developed and

tested. We also consider other estimators and the errors associated by using a mixed estimator.

II. METHOD

A. Fixed-Node Diffusion Monte Carlo (FN-DMC)

Diffusion Monte Carlo is a projector method that evolves a trial wavefunction with the exact Hamiltonian in imaginary time and projects out the ground-state wavefunction in the infinite time limit. Typically the fixed-node approximation is introduced to overcome the sign-problem suffered in fermion simulations. If the trial wavefunction has the same nodal surface as the exact ground-state wavefunction, the final ground-state energy will be exact. It should be noted that even with an approximate nodal surface, FN-DMC will still produce an excellent approximation of the exact ground-state energy including exact description of correlations between particles. In addition, since the exact Hamiltonian is used, the FN-DMC method is variational, that is, even when the nodes of the trial wavefunction are not exact the result will be a rigorous upper bound to the exact ground-state energy.

Due to advances in wave function optimization, it is now possible to optimize thousands of wave function parameters simultaneously with variational Monte Carlo. However, in these benchmark studies, the authors always worked within the adiabatic assumption, i.e., only the electronic Hamiltonian is used in evolving the trial wavefunction in imaginary time, while the ions are "clamped" to their equilibrium positions. Such an assumption is not fundamentally required by FN-DMC. Its inclusion is

mostly due to a lack of mean field theories that include non-adiabatic effects. Although there is significant effort in the quantum chemistry community to develop such methodology, until a standardized package is developed we will have to rely on modification of the QMC algorithm itself to include non-adiabatic effects. To this end, we will use the technique developed by Tubman *et al.* [1] to construct a high quality all-electron-ion wavefunction from an optimized all-electron wavefunction.

B. Electron Wavefunction and Optimization

We followed the basic strategies of Umrigar *et al.* [2, 3] and Needs *et al.* [4, 5] in generating our all-electron wavefunctions. The initial guess for the wavefunction is generated from Complete Active Space Self-Consistent Field (CASSCF) [6, 7] calculation using the quantum chemistry package GAMESS [8]. The optimized orbitals are then used in a Second Order Configuration Interaction (SOCI) calculation to generate a series of Configuration State Functions (CSF). This process is described in more detail in Ref. [9]. The multi-CSF expansion of the wavefunction generated by GAMESS can be expressed in the following form

$$\Psi_{SOCI}(\vec{r}) = \sum_{i=1}^{N_{CSF}} \alpha_i \phi_i(\vec{r}), \qquad (1)$$

where $\vec{r}$ refers to the spacial coordinates of all the electrons. $\phi_i(\vec{r})$ are the CSF generated from SOCI. We used the cc-pV5Z basis for all the atomic systems but switched to Roos Augmented Triple Zeta ANO basis for molecular systems due to the limited ability to handle a large number of basis elements in GAMESS. Both basis sets are taken from Basis Set Exchange [10].

A Jastrow factor $J(\vec{r}, \vec{\beta})$, in the form of a B-spline with values $\vec{\beta}$ on a linear grid, is then added to the wave function to correlate electron motion and smooth out the divergence in the local energy near the ions by imposing the cusp condition [11]. Our Jastrow factor contains one electron-ion term, two electron-electron terms (one for same spin electrons, one for opposite spin electrons) and two electron-electron-ion terms. The actually wave function being optimized is then

$$\Psi_e(\vec{r}) = e^{J(\vec{r},\vec{\beta})} \sum_{i=1}^{N_{CSF}} \alpha_i \phi_i(\vec{r}) \qquad (2)$$

We optimized the CSF and Jastrow coefficients $\vec{\alpha}, \vec{\beta}$ simultaneously with QMCPACK [12].

C. Electron-Ion Wavefunction

Once a satisfactory electronic wave function has been obtained, we construct the electron-ion wave function us-
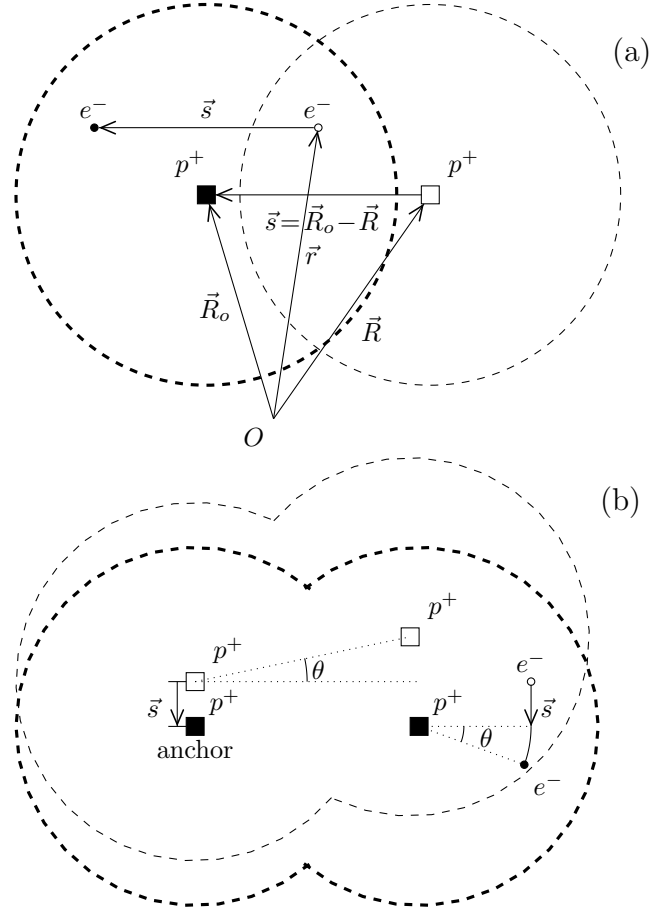

FIG. 1: Dragged node approximation: **(a)** For hydrogen atom, we assume the entire wavefunction shifts with the ion. This process can be visualized by following a contour of the wavefunction. The thick dashed circle represents a contour of the electron wavefunction when the proton is at its reference position $\vec{R}_o$ and the thin dashed circle represents the same contour when the proton has moved to a new position $\vec{R}$. To evaluate the ion-dependent electron wavefunction $\bar{\psi}_e(\vec{r}, \vec{R})$, we simply map the electron to its proper place in the reference wavefunction $\psi_e(\vec{r})$. That is, $\bar{\psi}_e(\vec{r}, \vec{R}) = \bar{\psi}_e(\vec{r} + \vec{s}, \vec{R}_o) = \psi_e(\vec{r} + \vec{s})$ where $\vec{s}$ is the shift required to put the proton back to its reference position. **(b)** For H_2^+, we pick one of the protons as an "anchor" and approximate the new wavefunction by dragging the reference wavefunction with the "anchor" proton. We also rotate the wavefunction to align its axis of symmetry with the orientation of the two protons.

ing the ansatz introduced by Tubman *et al.* [1]:

$$\Psi_{ei}(\vec{r}, \vec{R}) = \psi_I(\vec{R}) \bar{\psi}_e(\vec{r}, \vec{R}), \qquad (3)$$

where $\vec{R}$ includes spatial coordinates of all ions. The ion wave function consists of simple products of Gaussian wave functions over each nuclei pair.

$$\psi_I(\vec{R}) \propto \prod_{i,i<j} e^{-a(|\vec{R}-\vec{R}_j|-b_{ij})^2}, \qquad (4)$$

where a is a contraction coefficient for the ion wave function that we optimize for each system and b_{ij} are taken

to be the equilibrium distances between the nuclei in the adiabatic limit. Notice the new electron wavefunction $\bar{\psi}_e$ depends on both the electron and the ion positions. In general $\bar{\psi}_e(\vec{r}, \vec{R}) \neq \psi_e(\vec{r})$, but we do have $\bar{\psi}_e(\vec{r}, \vec{R}_o) = \psi_e(\vec{r})$, where $\vec{R}_o$ are the ion positions used in the creation of the $\psi_e(\vec{r})$. The most straight-forward way to obtain $\bar{\psi}(\vec{r}, \vec{R})$ is to repeat the process described in the previous section for every new ion positions $\vec{R}$. However, such an approach would be horrendously expensive. To alleviate the computational cost, Tubman *et al.* proposed a "Dragged Node Approximation" [1], where the contours (including the nodal surface) of $\psi_e(\vec{r})$ are dragged along the ions $\vec{R}$ to create $\bar{\psi}(\vec{r})$. In Fig. 1 we demonstrate this strategy for the simple cases of a hydrogen atom and a H_2^+ molecular ion. For atoms, this "dragged-node" process is equivalent to re-running a quantum chemistry calculation and re-optimizing the wavefunction at each new ion position. However, for diatomic molecules, since the distance between ions fluctuates, the two processes will produce slightly different wavefunctions. It is also important to note that the trial wavefunction (3) is still in Born-Oppenheimer form for each set of ion coordinates, that is we are essentially using the Born-Oppenheimer wavefunction as the starting point of FN-QMC. Nevertheless, without modifications to the Hamiltonian, FN-DMC will automatically include non-adiabatic effects not present in the trial wavefunction and the process remains variational.

Although the dragged-node technique is developed with atomic and diatomic systems in mind, it is not difficult to generalize it for use in larger systems or even apply to parts of a bigger system, e.g., treating light ions as quantum particles and heavy ions as "clamped". For a system of more than 3 particles, a general fitting procedure [13] can be done to determine the transformation needed to put the ions back to their reference positions. This is similar to the process of protein structure alignment implemented in some well-known biophysics software such as VMD [14]. Once the transformation is determined, we can map each electron individually and evaluate the wavefunction with moved ions using the reference wavefunction as was done for atoms and diatomics. One complication occurs when the ions become degenerate (when there are more than two protons with the same spin for example). In this case one has to explicitly anti-symmetrize the wavefunction of the ions, Eq. (4), in a manner similar to what is done for the electron wavefunction (Slater determinant).

III. RESULTS AND DISCUSSION

A. Ground State Energies

Ground state energies were calculated for first row atoms and ions with and without the adiabatic assumption, see Table I. The first row of Table I lists the level of

CASSCF calculation we used to generate the all-electron wavefunction guess. We first performed a CAS(m,n) calculation, meaning that we distribute m electrons into n active orbitals, with the ground-state equilibrium geometries taken from experimental data [16]. The MCSCF optimized orbitals are then used in a SOCI calculation that includes single and double excitations of the m electrons into all of the available valance orbitals provided by the basis. The SOCI ground state CSF $\phi_0(\vec{r})$ always dominates the expansion (with $\alpha_0 > 0.95$). Nevertheless, we include all CSFs with coefficients bigger than some cutoff ϵ to lend reasonable flexibility to the wavefunction during optimization. The choice of ϵ is somewhat arbitrary. We wish to included as many CSFs as possible to maximize the flexibility of the wavefunction. However, the inclusion of too many CSFs with small expansion coefficients introduces unnecessary noise into the system and requires a large number of samples in the optimization step to reach our desired accuracy. Therefore, we have chosen ϵ to restrict the number of CSFs in the wave function to be ~1000 in all systems to maintain a balance between the flexibility and the cost of optimization. In all of the atoms and molecules tested, this criteria results in an ϵ of $\sim 0.0001 - 0.001$, and the sum of coefficients squared of the included CSFs gives $\sum a_i^2 > 0.999$ in all cases. Optimization was performed with 6×10^6 statistically independent samples and we chose a cost function consisting of equal parts average local energy and reweighted variance. We found this choice of cost function to produce slightly better wavefunctions than a highly biased one, albeit the differences are small and are most likely insignificant at the DMC level.

We also performed timestep extrapolation for all of the tested systems. Five timesteps from 0.005Ha^{-1} to 0.001Ha^{-1} were used for all systems in the adiabatic FN-DMC. A smaller timestep (0.0005Ha^{-1}) is used for systems with 7 or more electrons. For such small timesteps almost all DMC runs have $> 99\%$ acceptance rate, thus we expect the timestep error to be very small. Indeed, for systems with fewer than 7 electrons, the DMC energies at all tested timesteps agree within error bars, only larger systems exhibit linear extrapolation behavior.

The adiabatic ground state energies of atoms are in perfect agreement with the most recent QMC benchmark study [5]. The non-adiabatic ground-state energies for Be and B ($-14.66643(2)$Ha and $-24.65244(3)$Ha) are in good agreement with ECG results (-14.66643544Ha [17] and -24.652598Ha [18]). Even though we used massive multi-determinant expansions (~ 1000 CSF) in our study whereas Seth *et al.* [5] used moderately-sized multi-determinant expansions (~ 100 CSF) with a backflow transformation, we both obtain almost the same DMC energies, but with very different wavefunctions.

Similar calculations were performed for diatomic systems, Table II, and the results are in excellent agreement with the sophisticated coupled cluster study [19]. It is important to note that with our method, the only included non-adiabatic effects are the zero point motion of

TABLE I: Ground state energies for atoms and ions, and the ionization energies: Fixed-Node DMC results of this work (FN-DMC) for atoms and ions with and without the adiabatic assumption. The ionization potentials (IP) are reported in the last section of the table with the experimental values at the end. Energies are given in units of Hartree.

Atom	Li(^{2}S)	Be(^{1}S)	B(^{2}P)	C(^{3}P)	N(^{4}S)	O(^{3}P)	F(^{2}P)
			adiabatic				
FN-DMC	-7.478056(4)	-14.66732(1)	-24.65377(1)	-37.84449(2)	-54.58858(3)	-75.06576(4)	-99.7316(1)
Seth DMC [5]	-7.478067(5)	-14.667306(7)	-24.65379(3)	-37.84446(6)	-54.58867(8)	-75.0654(1)	-99.7318(1)
Davidson 1993 [15]	-7.47807	-14.66736	-24.65391	-37.8450	-54.5892	-75.0673	-99.7339
			non-adiabatic				
FN-DMC	-7.47742(1)	-14.66643(2)	-24.65244(3)	-37.84277(6)	-54.58655(8)	-75.0631(1)	-99.7290(4)
Ion	Li$^+$(^{1}S)	Be$^+$(^{2}S)	B$^+$(^{1}S)	C$^+$(^{2}P)	N$^+$(^{3}P)	O$^+$(^{4}S)	F$^+$(^{3}P)
			adiabatic				
FN-DMC	−7.279919(4)	-14.324753(6)	-24.34884(1)	-37.43075(2)	-54.05376(3)	-74.56588(4)	-99.0913(1)
Seth DMC [5]	-7.279914(3)	-14.324761(3)	-24.34887(2)	-37.43073(4)	-54.05383(7)	-74.56662(7)	-99.0911(2)
Davidson 1993[a] [15]	-7.27999	-14.3249	-24.3489	-37.4312	-54.0552	-74.5668	-99.0937
			non-adiabatic				
FN-DMC	-7.2793(1)	-14.32386(2)	-24.34750(3)	-37.42904(4)	-54.05182(9)	-74.56336(8)	-99.0885(3)
			adiabatic				
IP (FN-DMC)	0.19814(1)	0.34256(2)	0.3049(3)	0.4138(5)	0.53475(8)	0.500(1)	0.640(1)
			non-adiabatic				
IP (FN-DMC)	0.1981(1)	0.34257(2)	0.3049(3)	0.4137(5)	0.53473(8)	0.500(1)	0.640(1)
IP (Exp.) [15]	0.19808	0.3425	0.30502	0.413797	0.533967	0.500526	0.640173

[a] The ionic ground state energies are calculated by adding ionization potentials in Table XII to the atomic ground state energies in Table XI from Ref. [15].

the nuclei and any correlation that may exist among the quantum particles. We do not take into account spin-orbit coupling or relativistic effects. Therefore, we subtracted the corresponding corrections from the values of Ref. [19]. Specifically, we took the reference energies from the last column of Table VI of Ref. [19] and subtracted the corrections in the ΔE_{SR} and SO columns for comparison with our non-adiabatic energies. On the other hand, for the comparison with our adiabatic energies we further subtracted the DBOC and ZPE corrections.

It should be emphasized that in principle our method is much simpler, since there is no need for separate computations for each correction factor, and thus, no addition of uncertainties. Further, the uncertainties in our calculations are statistically controlled and may be reduced by increasing computation time.

B. Ionization Energies

The ionization energies are listed at the end of Table I and they agree well with experimental results. Notice that even though ground state energies change significantly with the inclusion of non-adiabatic effects, the ionization energies match perfectly with or without the adiabatic assumption. This suggests that for atomic systems, the gradient coupling between electron and ion motions is indeed negligible. The difference in ground state energies can be entirely attributed to the zero point motion of the nuclei. Physically, this means that for all first row atoms, the outer most electron is perfectly screened

from the nucleus and all of the energy required for its removal can be attributed to its interaction with the rest of the electrons in the atom.

In order to obtain the electron affinity of LiH we also calculated the he ground state energy of LiH$^-$, which in the adiabatic limit at the DMC level is −8.08220(2)Ha, and with non-adiabatic effects included we get −8.07811(3)Ha. Our non-adiabatic result is in good agreement with a previous ECG study [20] which reported a value of −8.07856887Ha. We report an electron affinity of 0.01191(4)Ha which is very close to the ECG prediction of 0.012132(2)Ha and agrees with experiment 0.0126(4)Ha up to the mHa level. It should be noted that the authors of [20] mislabeled the columns for ground state energies of LiH$^-$ and LiD resulting in a miss-citation in [21].

C. Atomization Energies

The ground state energies of first row hydrides are reported in Table II. The energies calculated in the adiabatic limit are on par and sometimes better than the best available quantum chemistry results [22–24]. The energies calculated without the adiabatic assumption are in excellent agreement with state-of-the-art quantum chemistry calculations performed with ECG where available (LiH, BeH and BH). In the case of simple hydrides, non-adiabatic effects do make a noticeable contribution to the atomization energy. This is possibly due to the presence of the light weighted proton.

TABLE II: Ground state energies and atomization energies: Fixed-Node DMC results of this work for all first row hydrides with and without the adiabatic assumption. Energies are given in units of Hartree.

Molecule	LiH ($^1\Sigma^+$)	BeH ($^2\Sigma^+$)	BH ($^1\Sigma^+$)	CH ($^2\Pi$)	OH ($^2\Pi$)	HF ($^1\Sigma^+$)
			adiabatic			
E (this work)	-8.070521(7)	-15.24793(1)	-25.28868(2)	-38.4781(1)	-75.7352(1)	-100.4556(2)
E_{ref} [a] [15, 19, 22–24]	-8.07045	-15.247846	-25.287650	-38.4792(2)	-75.7382(2)	-100.4600(3)
			non-adiabatic			
E (this work)	-8.06620(2)	-15.24196(7)	-25.28103(4)	-38.4704(4)	-75.7237(4)	-100.4445(5)
ECG [17, 18, 20]	-8.0664371(15)	15.24203(10)	-25.2803(10)	N/A	N/A	N/A
			adiabatic			
D_e (this work)	0.092465(8)	0.08062(1)	0.13491(2)	0.13361(2)	0.16944(4)	0.2240(2)
Feller 2008[b] [19]	0.09262(5)	0.0809(4)	0.1354(2)	0.1342(2)	0.1709(2)	0.2258(3)
			non-adiabatic			
D_0^0 (this work)	0.08905(2)	0.07580(7)	0.12886(5)	0.1279(7)	0.1610(4)	0.2158(6)
Feller 2008[c] [19]	0.08940(5)	0.0761(4)	0.1299(2)	0.1276(2)	0.1622(2)	0.2166(3)
Exp. [16]	0.08874(38)	0.0826(11)	0.1281(37)	0.1275(5)	0.1622(1)	0.2158(3)

[a] For the smaller systems (LiH, BeH and BH), ECG studies provide the best reference energies. For CH, OH and HF, we combined the atomic energies in Ref. [15] with the atomization energies in [19] to produce the reference energies.

[b] The non-relativistic atomization energy in the adiabatic limit are calculated by subtracting the scalar relativistic, spin-orbit coupling and zero-point energy corrections from the reference energies in Table VI of Ref. [19].

[c] Here only the scalar relativistic and spin-orbit coupling corrections are subtracted.

IV. MOVING THE NUCLEI

The results of this work given in Tables I and II were obtained from simulations where we moved the nuclei as often as the electrons, i.e., we have used the same time-step for each particle. However, we could also use different sized time-steps for each different particle species as long as they are, e.g., multiples of the smallest time-step. Due to the Trotter expansion [?] this only affects the diffusion term in the diffusion Monte Carlo method, not the branching part. Thus, while applying the kinetic projection operator of the electrons for M times with time-step τ, a heavier particle can use a kinetic projector with time-step $\beta = M\tau$, which is applied only once. Our numerical tests with LiH molecule show that even with $M = 1000$ for the proton, and $M = 4000$ for the Li nucleus the results coincide with those shown in Table II, in which that nuclei were moved as often as the electrons. However, we believe that for the Li nucleus M could be larger, since in the diffusion term the exponential has a prefactor of $m/2\tau$. Therefore, it is possible that M could be roughly equal to the mass of the particle, since then the prefactor $m/2M\tau$ would roughly be equal to the one found accurate for the electrons.

The major benefit of this "multi-time-stepping" procedure is that going beyond the dragged-node approximation one needs to calculate on-the-fly updates for the electronic wave function each time the nuclei are moved. Thus, the possibility to make external program calls only every thousand steps in case of nonadiabatic hydrogen, and every four thousand (or even ten thousand) steps in case of Li nuclei will enable even more accurate calculations for more complex systems.

V. CONCLUSION

We calculated the ground-state energies of first row atoms and their corresponding ions and hydrides to an accuracy of 0.1mHa both with and without the adiabatic assumption. We found the ionization energies of the atoms to be independent of the adiabatic assumption, suggesting that either the energy difference between the adiabatic and non-adiabatic ground states is entirely due to the zero point motion of the nuclei or the coupling between the nucleus and electrons is not important in the ionization process. The atomization energies of simple hydrides, however, were significantly different in the adiabatic than in the non-adiabatic limit. This is most likely due to the presence of the light nucleus, i.e. the proton, in the molecule. We showed that it is necessary to include non-adiabatic effects to accurately predict the experimental values of atomization energies for these simple hydrides.

These calculations also verified the validity of the "dragged-node" approximation, namely it does indeed produce a high quality electron-ion trial wavefunction from a good electron wavefunction. This technique also has the potential to solve interesting larger-scale problems due to its ease of implementation as well as the polynomial scaling in computational time with respect to the number of electrons. As discussed at the end of the Method section, this technique can be generalized quite easily to deal with larger systems. In addition, we are able to offer similar levels of accuracy compared to the most sophisticated quantum chemistry methods (coupled cluster and ECG) while maintaining a reasonable level of computational and human cost.

VI. ACKNOWLEDGMENT

[1] N. M. Tubman, I. Kylänpää, S. Hammes-Schiffer, and D. M. Ceperley, Phys. Rev. A **90**, 042507 (2014), URL http://link.aps.org/doi/10.1103/PhysRevA.90.042507.

[2] C. J. Umrigar, J. Toulouse, C. Filippi, S. Sorella, and R. G. Hennig, Phys. Rev. Lett. **98**, 110201 (2007), URL http://link.aps.org/doi/10.1103/PhysRevLett.98.110201.

[3] J. Toulouse and C. J. Umrigar, The Journal of Chemical Physics **128**, 174101 (2008), URL http://scitation.aip.org/content/aip/journal/jcp/128/17/10.1063/1.2908237.

[4] M. D. Brown, J. R. Trail, P. Lpez Ros, and R. J. Needs, The Journal of Chemical Physics **126**, 224110 (2007), URL http://scitation.aip.org/content/aip/journal/jcp/126/22/10.1063/1.2743972.

[5] P. Seth, P. L. Ros, and R. J. Needs, The Journal of Chemical Physics **134**, 084105 (2011), URL http://scitation.aip.org/content/aip/journal/jcp/134/8/10.1063/1.3554625.

[6] G. Chaban, M. Schmidt, and M. Gordon, Theoretical Chemistry Accounts **97**, 88 (1997), cited By 46, URL http://www.scopus.com/inward/record.url?eid=2-s2.0-0031285817&partnerID=40&md5=e4a489f42a71cc286d31d63cf07fa630.

[7] A. Szabo and N. S. Ostlund, *Modern Quantum Chemistry* (McGraw-Hill, Inc., 1989).

[8] M. W. Schmidt, K. K. Baldridge, J. A. Boatz, S. T. Elbert, M. S. Gordon, J. H. Jensen, S. Koseki, N. Matsunaga, K. A. Nguyen, S. Su, et al., Journal of Computational Chemistry **14**, 1347 (1993), ISSN 1096-987X, URL http://dx.doi.org/10.1002/jcc.540141112.

[9] B. K. Clark, M. A. Morales, J. McMinis, J. Kim, and G. E. Scuseria, The Journal of Chemical Physics **135**, 244105 (2011), URL http://scitation.aip.org/content/aip/journal/jcp/135/24/10.1063/1.3665391.

[10] K. L. Schuchardt, B. T. Didier, T. Elsethagen, L. Sun, V. Gurumoorthi, J. Chase, J. Li, and T. L. Windus, Journal of Chemical Information and Modeling **47**, 1045 (2007), pMID: 17428029, http://dx.doi.org/10.1021/ci600510j, URL http://dx.doi.org/10.1021/ci600510j.

[11] T. Kato, Communications on Pure and Applied Mathematics **10**, 151 (1957), ISSN 1097-0312, URL http://dx.doi.org/10.1002/cpa.3160100201.

[12] QMCPACK, *www.qmcpack.org*.

[13] W. Kabsch, Acta Crystallographica Section A **32**, 922 (1976), URL http://dx.doi.org/10.1107/S0567739476001873.

[14] W. Humphrey, A. Dalke, and K. Schulten, Journal of Molecular Graphics **14**, 33 (1996).

[15] M. Puchalski and K. Pachucki, Phys. Rev. A **78**, 052511 (2008), URL http://link.aps.org/doi/10.1103/PhysRevA.78.052511.

[16] *Nist computational chemistry comparison and benchmark database, nist standard reference database number 101, release 16a, august 2013. editor: Russell d. johnson iii, http://cccbdb.nist.gov/.*

[17] S. Bubin and L. Adamowicz, The Journal of Chemical Physics **126**, 214305 (2007), URL http://scitation.aip.org/content/aip/journal/jcp/126/21/10.1063/1.2736699.

[18] S. Bubin, M. Stanke, and L. Adamowicz, The Journal of Chemical Physics **131**, 044128 (2009), URL http://scitation.aip.org/content/aip/journal/jcp/131/4/10.1063/1.3195061.

[19] D. Feller, K. A. Peterson, and D. A. Dixon, The Journal of Chemical Physics **129**, 204105 (2008), URL http://scitation.aip.org/content/aip/journal/jcp/129/20/10.1063/1.3008061.

[20] S. Bubin, L. Adamowicz, and M. Molski, The Journal of Chemical Physics **123**, 134310 (2005), URL http://scitation.aip.org/content/aip/journal/jcp/123/13/10.1063/1.2047487.

[21] J. Mitroy, S. Bubin, W. Horiuchi, Y. Suzuki, L. Adamowicz, W. Cencek, K. Szalewicz, J. Komasa, D. Blume, and K. Varga, Rev. Mod. Phys. **85**, 693 (2013), URL http://link.aps.org/doi/10.1103/RevModPhys.85.693.

[22] W.-C. Tung, M. Pavanello, and L. Adamowicz, The Journal of Chemical Physics **134**, 064117 (2011), URL http://scitation.aip.org/content/aip/journal/jcp/134/6/10.1063/1.3554211.

[23] J. Koput, The Journal of Chemical Physics **139**, 104309 (2013), URL http://scitation.aip.org/content/aip/journal/jcp/139/10/10.1063/1.4820403.

[24] E. Miliordos and A. Mavridis, The Journal of Chemical Physics **128**, 144308 (2008), URL http://scitation.aip.org/content/aip/journal/jcp/128/14/10.1063/1.2902284.